Chapter III: Sputtering and secondary electron emission

References

[1] Handbook of Sputter deposition technology, Kiyotaka Wasa, Noyes publications, NJ 1992. ISBN: 0-8155-1280-5
[2] "Cold Plasma in Materials Fabrications", A. Grill, IEEE Press, NY(1993). ISBN: 0-7803-1055-1.
[3] "The Materials Science of Thin Films", M. Ohring, Academic Press, San Diego,1992. ISBN: 0-12-524990-X
[4] "Basic data of plasma Physics", S.C. Brown, AIP Press, N.Y., 1993. ISBN: 1-56396-273-X

1. Interactions of particles with surfaces

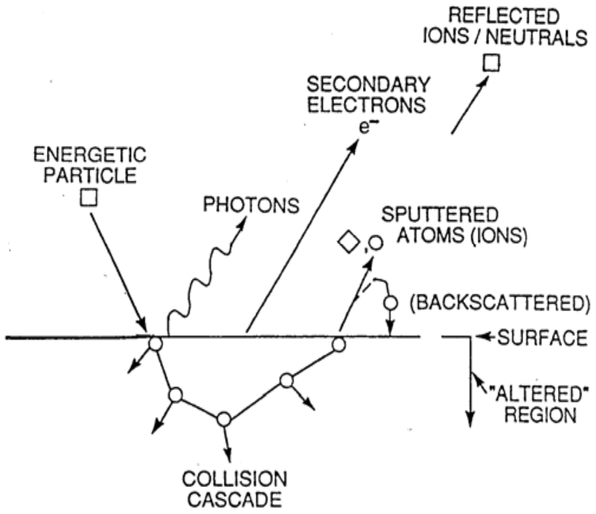

- First observed by Grove in a DC gas discharge in 1852. The cathode surface of a discharge tube was sputtered by energetic ions and deposited on the inner walls of the tube. At that time, it was regarded as an undesired phenomena. Today, it is widely used for surface cleaning and etching.
- Another phenomenon resulting from the particles bombardment of a surface is the secondary electron emission. It is observed for bombardment by ions, electrons, photons and neutrals. It plays a significant role in the glow discharges.

---

2. Sputter yield

$$S = \frac{\# atomsremoved}{\# incidentions}$$

S is function of:
- energy of incident particles,
- target material,
- incident angle of particles,
- crystal structure of the target.

2.1 Ion energy.

Threshold energy is in the range of 15 - 50 eV. It depends on the particular collision sequence involved.
E_{th} ↑↑ means primary recoil is produced in the first collisions and is ejected directly. E_{th} ↓↓ is for multiple sputtering collisions.
Maximum sputter yields are seen in region of about 10 keV.

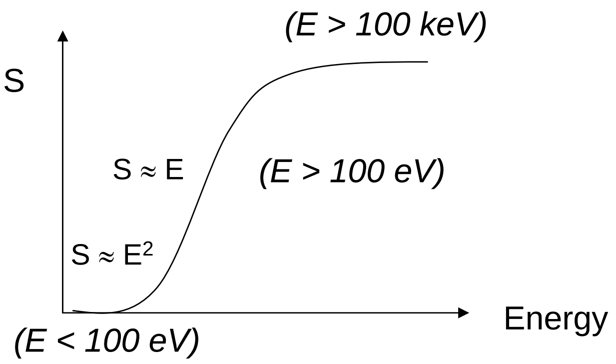

2. Sputter yield

Threshold values and sputtering yield for Ar bombardment [2,3]					
	Threshold (eV)	Ar$^+$ energy (eV)			
		200	300	500	600
C	-			0.12	
Al	13	0.35	0.65	1.05	1.24
Cr	22	0.67	0.87		1.3
Cu	17	1.1	1.59	2.35	2.3
Fe	20	0.53	0.76	1.1	1.26
Ni	21	0.66	0.95		1.52
Ge	25	0.5	0.74	1.1	
Si		0.18	0.31	0.5	0.53
Ti	20	0.22	0.33	0.51	0.58
V	23	0.31	0.41		0.7
Zr	22	0.28	0.41		0.75

---

2. Sputter yield

2.2 Incident ion, target material.

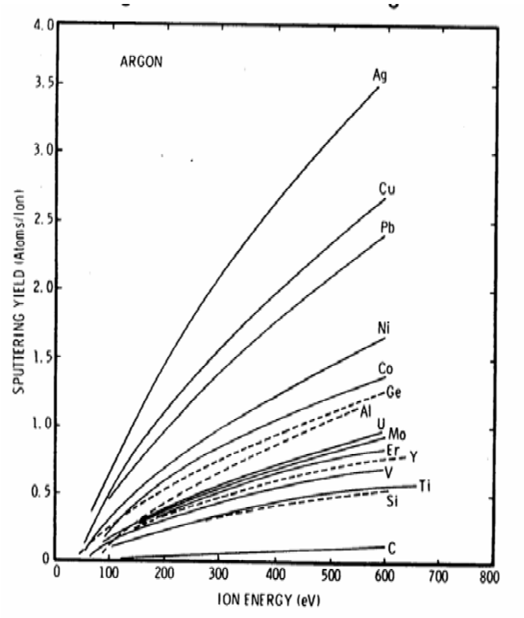

Sputtering yield versus incident atom and target (normal incidence) [2]						
	Ne			Ar		
	200	300	600	200	300	600
Al	0.24	0.43	0.83	0.35	0.65	1.24
Cu	0.84	1.2	2.0	1.1	1.59	2.3

2. Sputter yield

2.3 Angle of incidence and angular distribution

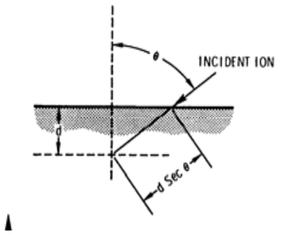

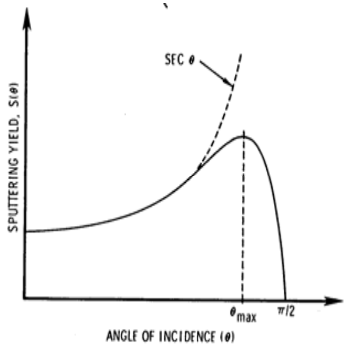

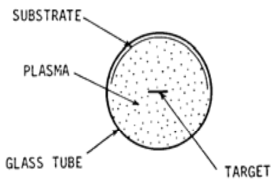

Figure 3.9: Experimental sputtering apparatus for the measurements of angular distributions (Wehner, Rosenberg, 1960 (19)).

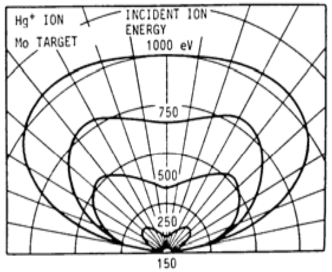

Figure 3.10: Angular distributions of sputtered particles from polycrystal target (Wehner, Rosenberg, 1960 19)).

---

2. Sputter yield

2.4 Crystal structure of the target

Sputtering yields and the angular distribution of the sputtered particles are affected by the crystal structure of the target.

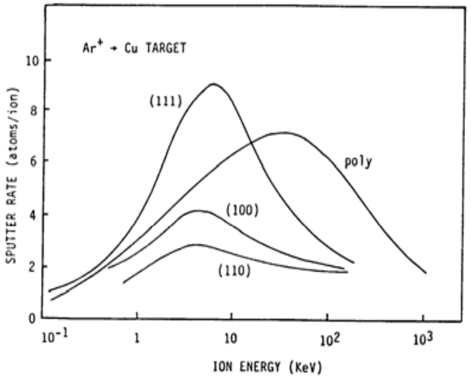

Figure 3.11: Energy dependance of the sputter yields of Ar⁺ on the (110), (100) and (111) planes of Cu (Roosendaal, 1983 (27)).

In very first approximation, this is related to the interplanar distance and the binding energy in the different planes.

When target is in liquid state, S ↓ of 20 - 30 %.

2. Sputter yield

2.5 Sputter yield of alloys

Experience have shown that chemical composition of deposited films sputtered from an alloy is very closed to that of the target. This suggests that sputtering is not governed by thermal processes, but by momentum transfer processes.

Suppose sputtering on a binary alloy target of A atoms and B atoms (n_A and n_B, $n=n_A + n_B$) with sputter yields S_A and S_B.

Target concentration: $C_A = n_A / n$ and $C_B = n_B / n$.

Flux of atoms A: F_A, Flux of atoms B: F_B.

$$\frac{F_A}{F_B} = \frac{S_A \cdot C_A}{S_B \cdot C_B}$$

If n_g atoms of gas impinge on the target, the total number of A atoms sputtered is $n_g C_A S_A$. Same for B

The surface concentration of the target is modified as:

$$\frac{C^*_A}{C^*_B} = \frac{C_A(1 - n_g S_A / n)}{C_B(1 - n_g S_B / n)}$$

2. Sputter yield

2.5 Sputter yield of alloys

If $S_A > S_B$, the surface is enriched in B atoms which now begins to sputter in greater profusion, i.e.

$$\frac{F^*_A}{F^*_B} = \frac{S_A C^*_A}{S_B C^*_B} = \frac{S_A C_A(1 - n_g S_A / n)}{S_B C_B(1 - n_g S_B / n)}$$

Progressive change in the surface target composition will alter the sputter flux ratio until it is equal to C_A/C_B, same as initial:

$$\frac{F^*_A}{F^*_B} = \frac{C_A}{C_B} \longrightarrow \frac{C^*_A}{C^*_B} = \frac{C_A S_B}{C_B S_A}$$

Ex: Target Permalloy film (80% Ni, 20 % Fe) at 600 eV:

$$\frac{C^*_A}{C^*_B} = \frac{80\,(1.26)}{20\,(1.52)} = 3.3$$

which is equivalent to 78 Ni and 23,6 Fe.

Remarks: This is in complete contrast to evaporation where deposit stoichiometry is totally lost.

2. Sputter yield

2.6 Sputtered atoms

2.6.1 Nature of sputtered species

Most sputtered material is ejected in the neutral atomic state. The fraction of the charged particles sputtered from clean metal and semiconductors is on the order of 10^{-4}, becoming larger for surfaces contaminated with strongly electropositive or electronegative species.

Polyatoms or clusters can also be formed, but in very low amount (< 1 %).

99.9 % of sputtered particles are neutral.

2.6.2 Energy distribution of sputtered particles.

$$E_{mpe} \approx E_B$$

E_B: Surface binding energy.

Surface binding energies for selected metals			
Element	E_B (eV/atom)	Element	E_B (eV/atom)
Mg	1.51	Ag	2.94
Al	3.39	Cd	1.16
Ni	4.44	W	8.79
Cu	3.48	Pt	5.85
Zn	1.35	Au	3.81
Nb	7.44	Pb	2.03

---

2. Sputter yield

2.6 Sputtered atoms

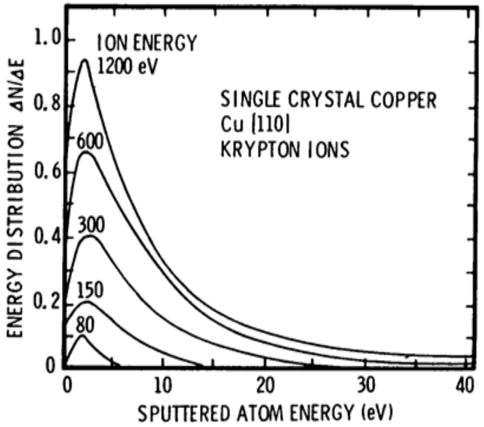

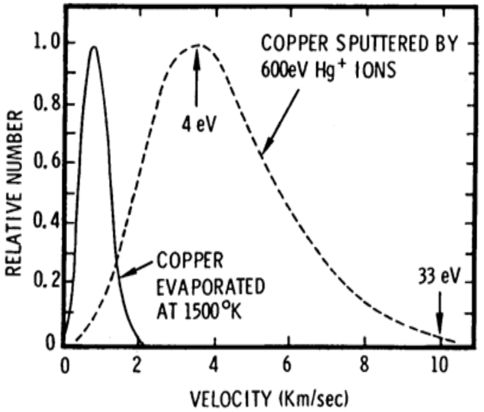

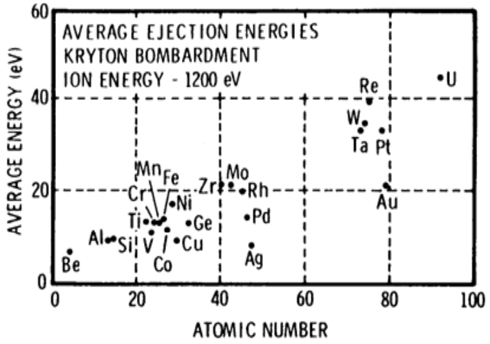

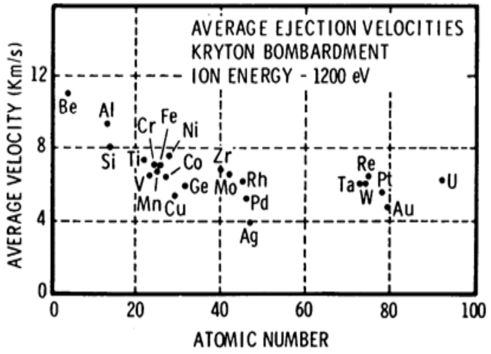

2. Sputter yield

2.7 Sputtering mechanisms

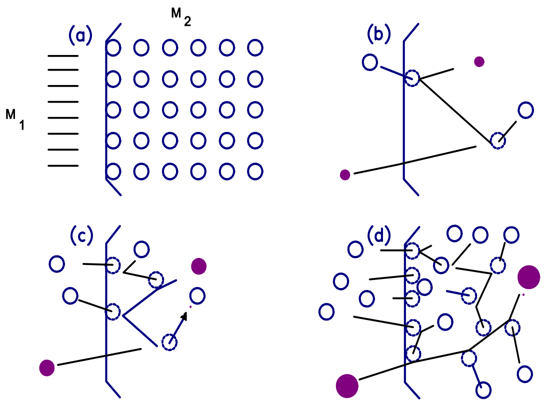

(b) Simple collisions: Low energy regime: incident ion stays under the surface, energy can be transferred to sputtered particles by incident ion
(c) Linear cascade: Sputtered particles have been mainly knocked by recoils from the targets. Appears for incident particles of several keV, and mean atomic weight.
(d) Thermal spike: Large amount of defaults are created inducing very high temperature (≈ evaporation T°). Appears for heavy ions of hundreds keV.

Regime (c) and (d) are found in Ion Implantation. Regime (b) is found in plasma sputtering.
In the energy range relevant to sputter deposition (< 1 keV), typical collision cascades are of radius 10 nm, and sputter ejection are due to collision cascades initiated within five atomic layers below the surface.

---

2. Sputter yield

2.7 Sputtering mechanisms

The maximum energy transferred T_m is:

$$T_m = \frac{4 M_1 M_2}{(M_1 + M_2)^2} E$$

It is max when $M_1 = M_2$.

Sigmund has established for E < 1 keV that:

$$S(E) = \frac{3}{4\pi^2} \frac{T_m}{U_B} \alpha$$

Sigmund has established for 1 < E < 10 keV that:

$$S(E) = 0.420 \alpha \frac{S_n(E)}{U_B}$$

Where U_B: heat of sublimation (eV),
α is a measure of the efficiency of momentum transfer in collisions
$S_n(E)$: Nuclear stopping power (fct Z_1,Z_2,M_1,M_2,Born-Mayer interaction potential, ...)

2. Sputter yield

2.7 Sputtering mechanisms

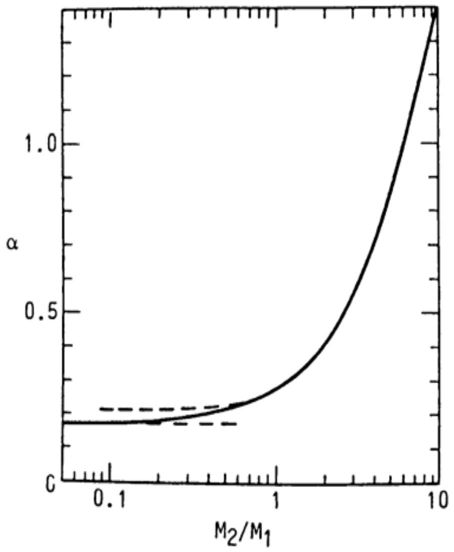

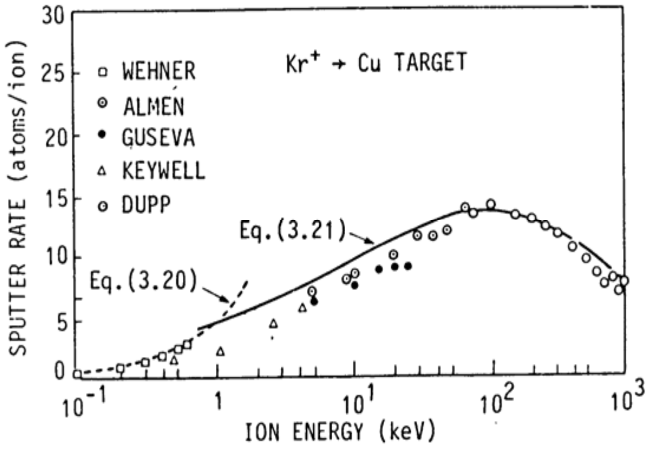

---

2. Sputter yield

2.8 Some data

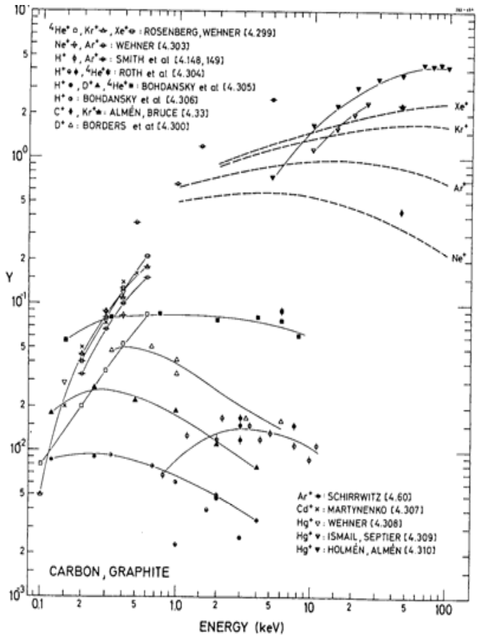

Fig. 4.5. Experimental sputtering-yield data for carbon. *Smith* et al. [4.147, 148] used evaporated targets, while *Holmén* and *Almén* [4.310], *Roth* et al. [4.304], and *Bohdansky* et al. [4.305, 306] used graphite from different suppliers, as did *Borders* et al. [4.300]. The remaining data have been obtained on unspecified "carbon"

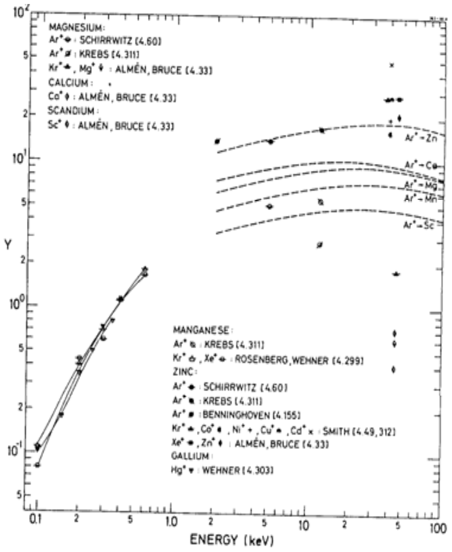

Fig. 4.6. Experimental sputtering-yield data for Mg, Ca, Sc, Mn, Zn, and Ga targets

2. Sputter yield

2.8 Some data

170 *H. H. Andersen* and *H.L. Bay*

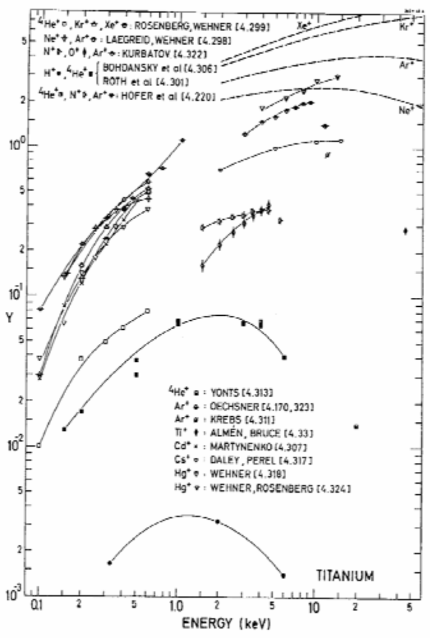

Fig. 4.9. Experimental sputtering-yield data for Ti targets

Sputtering Yield Measurements 171

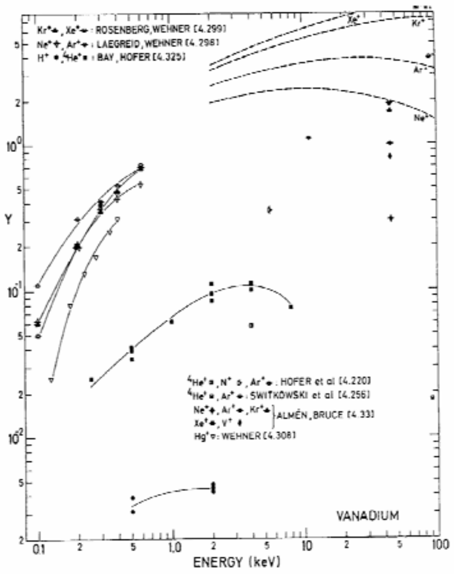

Fig. 4.10. Experimental sputtering-yield data for V targets

---

2. Sputter yield

2.8 Some data

172 *H. H. Andersen* and *H.L. Bay*

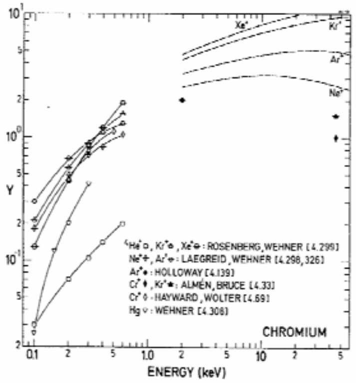

Fig. 4.11. Ex
sputtering-yield
Cr targets

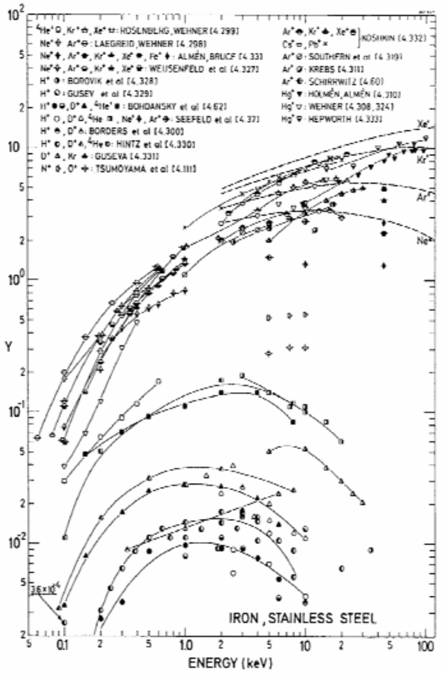

Fig. 4.12. Experimental sputtering-yield data for Fe and stainless-steel targets. *Borovik* et al. [4.328], *Guseva* [4.331], and *Gusev* et al. [4.329] used unspecified stainless steel; *Hepworth* [4.333] used EB 58 B, *Southern* et al. [4.319] and von *Seefeld* et al. [4.37] used SS316 stainless steel. Points by *Bohdansky* et al. [4.62] symbolized by ⊖ were measured on SS304, while filled-point data were obtained on SS316. The remaining points were measured on Fe

2. Sputter yield

2.8 Some data

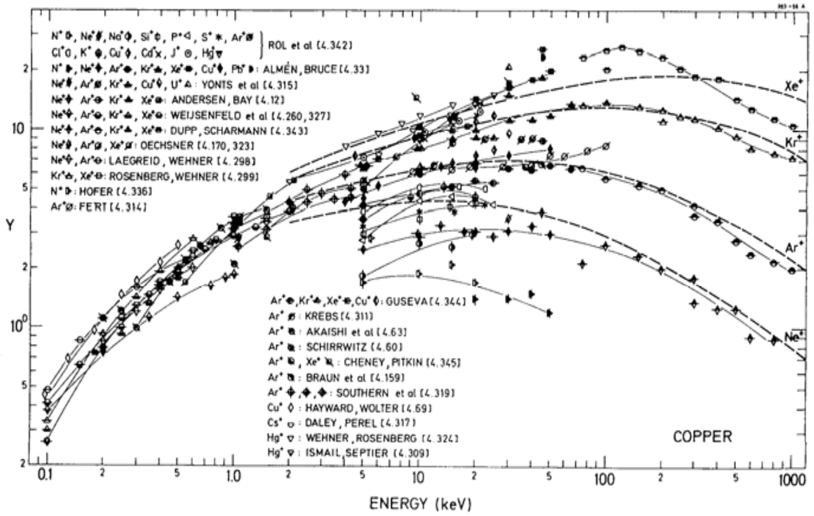

Fig. 4.16. Experimental sputtering-yield data for Cu targets. See also Fig. 4.15

---

3. Secondary electron emission

3.1 Electron bombardment

$$\delta = \frac{\#\, of\ emitted electrons}{\#\, of\ primary electrons}$$

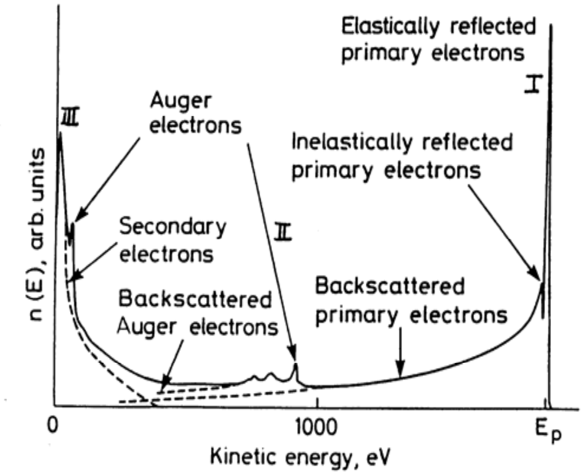

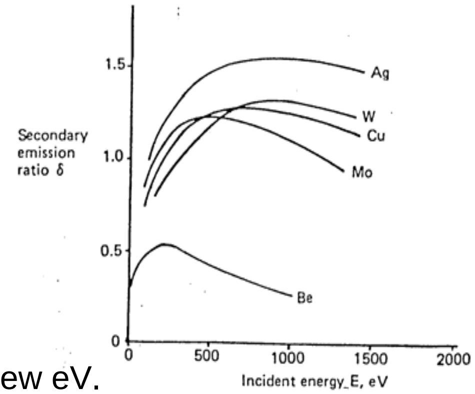

Rem: 2 nd Electron energy: few eV.

3. Secondary electron emission

3.1 Electron bombardment

δ_{max} and $V_{\delta max}$ [4]		
Element/Compounds	δ_{max}	$V_{\delta max}$ (800 V)
Ag	1.5	800
Al	1.0	300
C	1.0	300
Cu	1.3	600
Fe	1.3	350
Ni	1.3	550
W	1.4	600
Zr	1.1	350

---

3. Secondary electron emission

3.2 Ion bombardment

$$\gamma = \frac{\#\, of\ emitted electrons}{\#\, of\ primary ions}$$

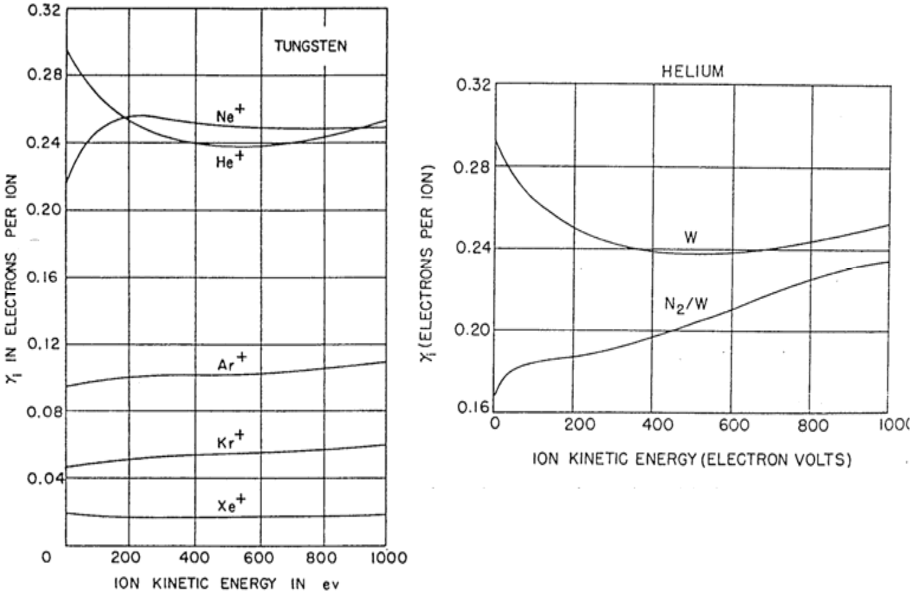

Rem:-Surface contamination plays a major role. This is very important in DC sputtering with a contaminated target (V-I characteristics. continuously changing).

- 2nd electron energy: few eV.
- γ for metals << 1 (typical: 0.2).
- γ for insulators > 1 (difficult to measure).

3. Secondary electron emission

3.3 Neutral bombardment

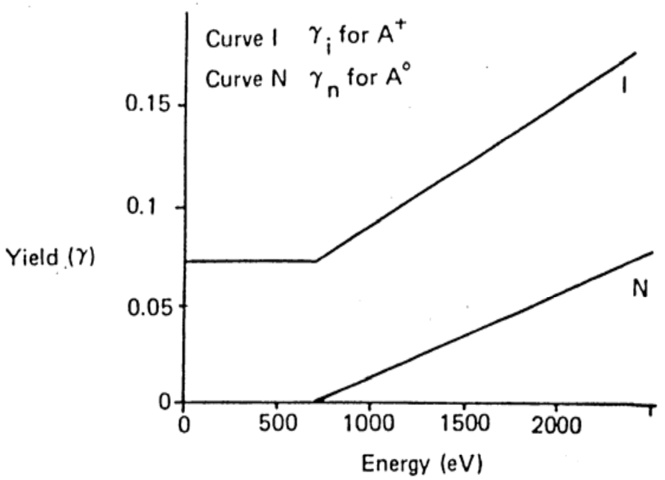

Secondary electron emission as a function of energy for argon ion and neutral atom bombardment of molybdenum (from Medved et al. 1963)

Rem: - In sheath of an electrode, energetic neutrals are produced through collisions of ions with neutrals. The neutral energies are a few hundred eV at most.

☞ Emission due to neutral collisions is probably negligible in cold plasma.

3.4 Photon bombardment

Typical photoelectric yield is 10^{-4} to 10^{-3} electron per photon, negligible in sputtering and cold plasma discharges.